



Neogene block rotation inside the dextral fault zone at the Adriatic-European collision zone: Reexamination of existing results

L. Žibret^{a,*}, G. Žibret^b

^a Slovenian National Building and Civil Engineering Institute (ZAG), Ljubljana, Slovenia

^b Geological Survey of Slovenia (GeoZS), Ljubljana, Slovenia

ARTICLE INFO

Keywords:

Collision zone
NW External Dinarides
Southern Alps
Paleostress tensor
Strike-slip zone
Block rotation

ABSTRACT

The study focused on the post-Middle-Miocene stress analysis within the dextral strike-slip zone of the Dinaric fault system in the collision zone between the European plate, the Adria microplate and the Pannonian Domain. Block rotations were studied by re-examination of available paleostress data and their spatial distribution. The results are in agreement with the existing block model of the area, indicating CCW rotations within blocks between the main strike-slip faults in which rotation angle increases from W to E. The improved kinematic model, which is proposed in this study, will contribute to the knowledge on the kinematics within the complex collision zones and improve the seismic hazard models.

1. Introduction

Crustal deformations in strike-slip environments are usually accompanied by block rotations in response to distributed shear. Rotation of blocks within strike-slip zones across the vertical axis may result in systematic rotation of the stress field close to zones of weakness within the crust (Homburg et al., 1997; Zoback et al., 1987). This can cause time-dependent crack formations which can affect the fault behaviour and might control fracture pattern of large earthquakes (Kissel and Laj, 1989). It is ununiformed process in time and occurs within weaker zones, which can accommodate elastic and non-elastic strain accumulation and can occur in various scales, up to several tens of kilometres, including decoupling within the upper crust (Kissel and Laj, 1989). Block rotations typically appear within the tips of damage zones, where antithetic faults and extension fractures form wedge-shaped patterns (Kim et al., 2003). Block rotations depend on the bulk sense of shear, similar as in the domino model (Axen, 1988). In oblique subduction zones slip partitioning commonly results in detachment of lithospheric blocks from the overriding plates. Block rotations and strain rates generated by locking at block-bounding faults are commonly identified by using GPS velocity vectors (McCaffrey, 2013; Wallace, 2004).

On structurally complex areas there are a lot of locally-driven movements, including rotations, which can be mistaken for important regional ones, and oppositely, regional trends can be blurred by a variety

of localized movements. To be able to distinguish between regional rotations from locally-driven ones it is important to study such rotational processes on very complex active tectonic areas by using multiple methods. This can improve the prediction of seismicity and other geologically-conditioned hazards, as well as it can improve our knowledge about kinematics of such movements. In this paper we demonstrate the problematics of “hidden” tectonic phases within structurally complex collision zones between three plates, i.e. the European plate, the Adria microplate and the Pannonian Domain (Fig. 1), which represents an important regional source of seismic activity and seismic hazard (Schmid et al., 2020). We upgraded the existing block model (Atanackov et al., 2021) by combining available data from two complimentary methods - paleostress analysis of fault-slip data (Fodor et al. 1998; Tomljenović and Csontos 2001; Bartel et al. 2014; Žibret and Vrabec 2016; Goričan et al. 2018) and paleostress data revealed by pebble orientation (Caputo et al., 2010).

1.1. Geological and geodynamic setting

The study area is located in the junction zone of three lithospheric units: the European plate, the Adria microplate and the Pannonian domain (Brückl et al., 2010) (Fig. 1). Geotectonic units of this area have been formed gradually during the Variscan orogenesis, Mesozoic rifting events and Neogene Dinaric and the Alpine orogeny. Ever since the Lower Jurassic, when the Adria microplate separated from the Africa

* Corresponding author.

E-mail address: lea.zibret@zag.si (L. Žibret).

<https://doi.org/10.1016/j.jseaes.2023.105723>

Received 1 March 2023; Received in revised form 12 May 2023; Accepted 19 May 2023

Available online 21 May 2023

1367-9120/© 2023 The Authors. Published by Elsevier Ltd. This is an open access article under the CC BY license (<http://creativecommons.org/licenses/by/4.0/>).

(Nubia) plate, the dominant geodynamic mechanism on the territory is N-directed movement of the Adria microplate and its collision with the European plate (Anderson and Jackson, 1987; Stojadinovic et al., 2022; Toljić et al., 2013). During the Miocene era, Adria-Europe deformation was divided between thrusting in the Dinaric and South-Alpine belts and an eastward escape of the ALCAPA block in front of the Adriatic indenter, north of the Periadriatic fault zone (Márton et al., 2002; Placer, 2008; Ratschbacher et al., 1991; Vrabcic and Fodor, 2006). Since the Miocene-Pliocene ages, the end of tectonic escape and the beginning of Adria counter clockwise (CCW) rotation launched activation of major strike-slip and contractional deformations between rigid Adria plate and the Periadriatic fault, accompanied by uplifting, folding, strike-slip basin formation, and, possibly, rigid-block rotation (Márton et al., 2002; Vrabcic and Fodor, 2006).

The most recent regional tectonic subdivision of the area is as a result of complex collisional processes between the Adria derived lithospheric units (Southern Alps, the Dinarides, ALCAPA mega-unit) and the European plate (the complex Tisza mega-unit) (Fig. 1; Schmid et al., 2020). The South Alpine thrust belt of Miocene S- to SE-verging thrusting on generally E-W striking thrust faults, corresponds to a late-stage retro-wedge of the Alpine collision, probably due to indentation of Adriatic lower crust into the European lithosphere (Fig. 1; Schmid et al., 1996). Part of the thrust belt in the northern and northeastern Italy is accommodating the ongoing CCW rotation of the Adria microplate (Galadini et al., 2005; Monegato and Poli, 2015). The External Dinarides system of NW-SE-striking fold-and-thrust belt is attributed to Late Jurassic to recent response to Adria under thrusting the Dinaric carbonate platform (Tari, 2002). The idea of late-stage wrenching of Adria vs. Alpine crust was proposed by Picha (2002) for the first time. An overlap of the Dinaric and younger Alpine structures was reported in the eastern Southern Alps (Goričan et al., 2018), on the boundary between the Southern Alps and the Dinarides (Placer and Car, 1997) and in the Internal Dinarides (van Gelder et al., 2015). The structures in the Central Adriatic area were affected by strong neotectonic deformation (Márton et al., 2022).

The territory north of the dextral strike-slip Periadriatic fault system is attributed to the Austroalpine unit (Schmid et al., 2020). Periadriatic fault system has accommodated the still-ongoing left-lateral extrusion of

the ALCAPA mega-unit, from 21 to 23 Ma on (Schmid et al., 2013; Ustaszewski et al., 2010). Structural pattern in the eastern part of the study area is mainly controlled by the interaction between the ALCAPA and accreted Tisza mega-unit near the Mid-Hungarian zone (Fig. 1). The Tisza mega-unit is composed of Mesozoic elements of Eurasian origin rocks, which were during the Paleogene-Miocene set in their recent configuration (Csontos and Nagymarosy, 1998; Handy et al., 2015; Schmid et al., 2020).

The Cenozoic motion of the Adriatic promontory behaved as a rigid prolongation of the Nubia Plate during most of the plate convergence period (Channell, 1996). Moreover, Moho maps suggest that the northern part of the Adriatic promontory should represent the most stable Neogene converging boundary in the Mediterranean (Faccenna et al., 2014).

The average velocity of Adria northward push is 2–4 mm/yr, accompanied by 30°/Myr CCW rotation around the pivot point, located in the western Alps (Márton et al., 2003; Serpelloni et al., 2016; Weber et al., 2010). Most of the predicted Adria-Europe motion is absorbed along the eastern boundary of the Adria microplate in the NW External Dinarides, where several individual »corridors« of uniform cumulative horizontal displacement/slip rates were identified (Fig. 1; Atanackov et al., 2021), which can be considered as individual blocks. According to determined GPS velocities the Periadriatic fault system accommodates approximately 1–2 mm/yr of dextral strike slip (Atanackov et al., 2021). The Dinaric fault system can be divided in two individual blocks; the western fault set which accommodates approximately 2.5 mm/yr, and the eastern fault set which accommodates approximately 1–2 mm/yr of dextral strike slip according to GPS velocities (Atanackov et al., 2021). Total GPS velocity derived slip rates of the order of ~0.5–1.0 mm/yr has been determined for the Mid-Hungarian fault system with the Sava compressive wedge, Balaton fault system and the Raba extensional fault system (Atanackov et al., 2021).

1.2. Neogene-recent tectonic phases

Inversion of the fault-slip data (Hancock, 1994; Sperner and Zweigel, 2010) allowed to distinguish four major successive Neogene tectonic phases in the NW External Dinarides: (i) NE-SW directed compression

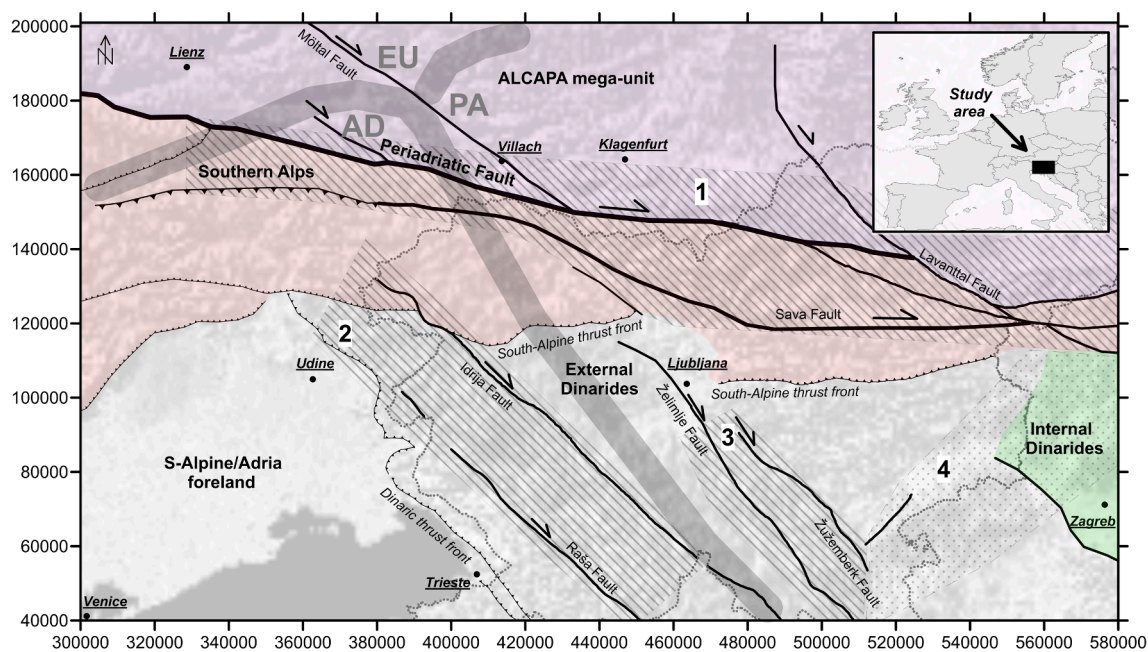


Fig. 1. Regional tectonic setting of the study area (Schmid et al., 2020, 2008) with indicated boundaries between the European plate (EU), the Adria microplate (AD) and the Pannonian Domain (PA) (Brückl et al., 2010). Approximate areas of cumulative horizontal displacement/slip rates across the study area is also indicated by hatching (Atanackov et al., 2021).

attributed to Late Eocene top-to-SW thrusting of External Dinarides (Žibret and Vrabec, 2016); (ii) NE-SW oriented tension attributed to Early to Middle Miocene back-arc extension in the Pannonian basin system that also affected the External Dinarides; (iii) approximately E-W oriented compression with approximately N-S oriented tension in a strike-slip stress regime attributed to Late Miocene short pulse of E-W directed compression, documented in parts of the Pannonian basin system; (iiii) approximately N-S oriented compression and approximately E-W oriented tension in a strike-slip stress regime attributed to the recent compressive/transpressive phase. Westward, in the eastern Southern Alps, the mean orientation of the σ_1 from the analyses of the pebbles' surfaces (shape and orientation of indented features) revealed four distinct Neogene-Quaternary deformational events, indicating plate convergence: (i) late Tortonian ($\sigma_1 = 313/0$), (ii) late Messinian-Early Pliocene ($\sigma_1 = 338/4$), (iii) Late Pliocene ($\sigma_1 = 314/3$), and (iiii) Early-Middle Pleistocene ($\sigma_1 = 160/3$) (Caputo et al., 2010). In the vicinity of the Periadriatic fault system of the Eastern Alps five main kinematic groups were recognized by paleostress investigations: (i) N-S compression; (ii) NW-SE compression; (iii) NE-SW compression, σ_3 changes gradually from subvertical to subhorizontal; (iiii) N-S compression; and (iiiii) NW-SE compression (Bartel et al., 2014). Moreover, the area south of the Periadriatic fault shows CCW rotation in respect to the area north of the Periadriatic fault, fitting with the CCW rotation of the Adria (Bartel et al., 2014). In the border zone between Alps, Dinarides and Pannonian basin, four main tectonic phases were recognised from Neogene-Quaternary structures from seismic lines, surface measurements and geological mapping: (i) ENE directed Early Miocene extension, partly synchronous with NW-SE shortening; (ii) NW-SE to WNW-ESE oriented extension, followed by a new generation of thrusts related to end Sarmatian shortening, (iii) Late Miocene E-W to WNW-ESE oriented extension (iiii) N-S to NW-SE oriented shortening from Late Pontium to present days (Dal Cin et al., 2022; Grützner et al., 2021; Heberer et al., 2017; Le Breton et al., 2017; Neubauer and Cao, 2021; Tomljenović and Csontos, 2001). Their kinematic model suggests a combination of Adria CCW rotation and N to NW shift of the Dinaric block in relation to the Alps (Tomljenović and Csontos, 2001). The reported Neogene paleostress and kinematic phases differ in various parts of the study area, corresponding to regional geometry of crustal discontinuities. On the other hand, the direction of Pliocene-Quaternary shortening has the same direction across the entire study area, which is well supported by earthquake focal mechanisms (Herak et al., 2009; Kastelic et al., 2013, 2008).

Although the transitional zone between the Alps and Dinarides represents a key region for understanding how the Adria microplate interacts with the stable Europe, there is still little known regarding the recent deformation pattern of the area, including dynamics of individual tectonic blocks. In this paper detailed spatial analysis of the post-Middle Miocene tectonic phases (Tomljenović and Csontos 2001; Caputo et al. 2010; Bartel et al. 2014; Žibret and Vrabec 2016) is presented and reinterpreted, considering the latest data on Adria-Europe plate dynamics (Schmid et al., 2020) and regional crust segmentation (Atanackov et al. 2021). Our results suggest an improved geodynamic model of Adria-Europe plate interaction, with an emphasis on block rotation. The model has potential application for seismological investigations of the area and for explaining fracture patterns of larger earthquakes, as well as it can serve as a case study to compare the results with similar complex situations in Asia and globally.

2. Methods

Within this study we reinterpreted paleostress tensors which were determined within the PhD research of the first author (Žibret, 2015, Žibret and Vrabec, 2016, Supplement 1), combined with data from studies collected in the neighbouring areas (Tomljenović and Csontos 2001; Caputo et al. 2010; Bartel et al. 2014) and data acquired from the field survey at the Pokljuka area in 2016–2018 (Goričan et al. 2018,

Supplement 2). Field work consisted of measurements of fault planes and associated slip indicators (Doblas, 1998; Petit, 1987; Sperner and Zweigel, 2010) in different stratigraphic units ranging in age from Mesozoic to Miocene (Fig. 2). Fault planes and associated slip indicators were detected on 128 locations, located mainly in the NW External Dinarides in Slovenia. Fault slip directions were detected on 70 locations, while on 58 locations there was a lack of reliable kinematic indicators. Relative chronology of displacements (older/younger) was also recorded during field examinations. It was based on the following criteria: (i) overprinting relationships between different families of fault striations on the same fault plane, (ii) crosscutting relationships between outcrop-scale and regional-scale faults, and (iii) ductile/brittle character of deformation, assuming ductile phases preceded brittle deformations. The time frame of palaeostress phases was roughly determined by the stratigraphic ages of rocks in which the relevant fault-slip data occurred. Analysed paleostress datasets (including raw data), a detailed description of data analysis protocol and field evidence for determination of relative ages of paleostress phases is available in the author's PhD thesis and related paper (Žibret, 2015; Žibret and Vrabec, 2016). Field work was done within the scope of PhD thesis by Žibret (2015) and the study of Goričan et al. (2018) for measurements on the Pokljuka area. Because this study focuses on younger tectonic phases (mainly Neogene), only data from post-Paleogene strata were processed. Phases related to older Dinaric orogeny and different Mesozoic records of extension were not included. Fault slip data and paleostress tensors were thus determined on 53 locations (Fig. 2) by using the total of 1404 measurements.

Inversion of fault-slip data (Hancock, 1994) was performed by T-Tecto software, which assumes the Gauss distribution of the angles between the slip direction and shear stress on the fault plane (Žalohar and Vrabec, 2007). The compatibility criteria of the fault slip with the stress tensor are defined by the Gauss function. The range of stress axes direction, which is described by one stress tensor, can vary depending on the expected homogeneity of the stress field. In the case of inhomogeneous stress field, high limit values of the compatibility measure ($\geq 30^\circ$) and the dispersion of the Gauss distribution ($\geq 60^\circ$) were set. The assumption in this study was that the inhomogeneous stress field was caused by the rotation of blocks within the dextral strike-slip fault zone. This is why low limit values of the compatibility measure ($\geq 15^\circ$) and the dispersion of the Gauss distribution ($\geq 30^\circ$) were used. Further data processing included statistical analyses of paleostress tensors, map preparations and comparison of obtained results with the latest studies (Atanackov et al., 2021; Goričan et al., 2018).

Statistical analyses were done by dividing the study area into 5 blocks and observing the orientations of paleostress tensors in each block separately. Blocks were determined according to findings of Atanackov et al. (2021), which defined three areas of relatively high and uniform dextral slip deformation. In this study we introduced 2 additional blocks, raising the total number of blocks to five:

- Block 1: the area between Raša and Idrija fault, as one of the most active dextral slip areas within the study area;
- Block 2: the area between Idrija and Želimplje fault, which is not very active according to Atanackov et al. (2021);
- Block 3: the area between Želimplje and Žužemberk fault, again a very active dextral strike slip area according to Atanackov et al., (2021);
- Block 4: area E of the Žužemberk fault and S of the Sava fault, named a Sava compressive wedge system and the W part of Balaton Fault system, representing a diffuse structural transition from the neighbouring fault systems;
- Block 5: the most western block which is positioned between the Raša fault and the Dinaric thrust front.

Determined paleostress tensor within 1 km buffer zone around the main faults were excluded from statistical analyses in cases of blocks 1, 2 and 4. However, no measurements far enough from the main fault zones in cases of blocks 3 and 5 were available, hence for these cases, all of the

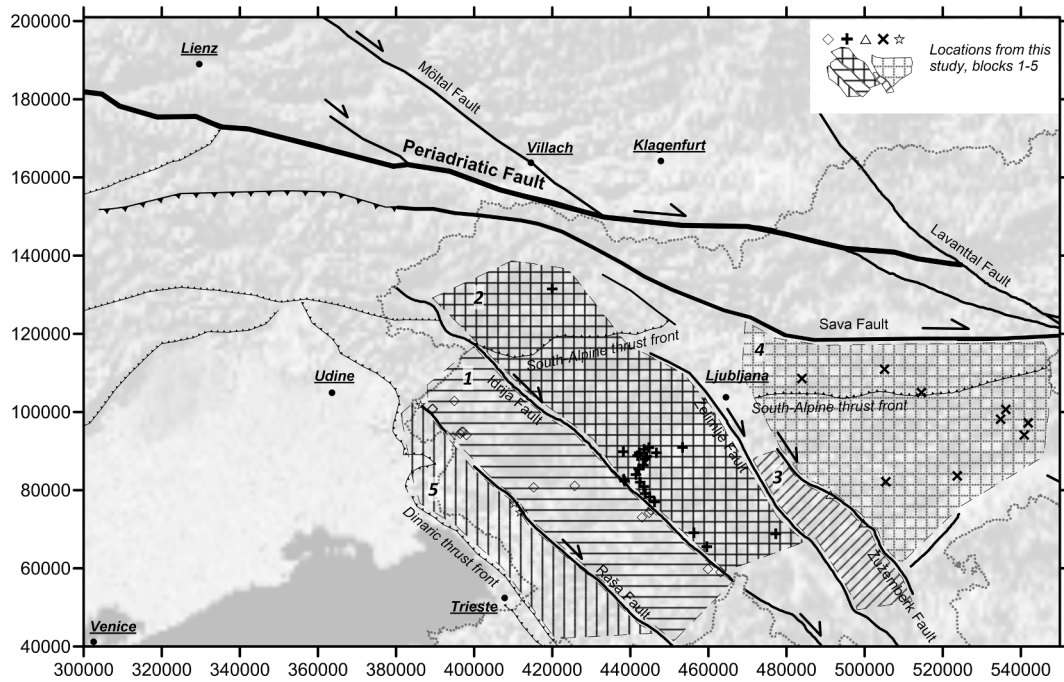


Fig. 2. Map of the main faults, measurement locations of tectonic-induced movements and separation of the study area on 5 blocks.

measurements were included. Paleostress data from the Sava fault zone were adopted after Fodor et al (1998).

3. Results

Fig. 3 presents the histogram of the main principle axes σ_1 and σ_3 orientations for all processed data combined. The principle orientation of σ_1 within this study is WNW-ESE, and of σ_3 it is NNE-SSW. Fig. 4 presents the relative relations of various phases based solely on field observations. The oldest phases were SW-NE thrust compression and NE-SW compression in strike-slip stress regime. Relatively younger phases are SW-NE and NW-SE tension and N-S oriented compression. Relatively youngest phases, which were determined based on field work observations, are N-S and E-W directed compressions in strike-slip stress regimes. This study was focused on reinterpretation of the youngest two paleostress phases. Fig. 5 presents orientations of the main stress tensors of the youngest stress regimes on a regional scale, combined with available studies (Bartel et al., 2014; Caputo et al., 2010; Tomljenović

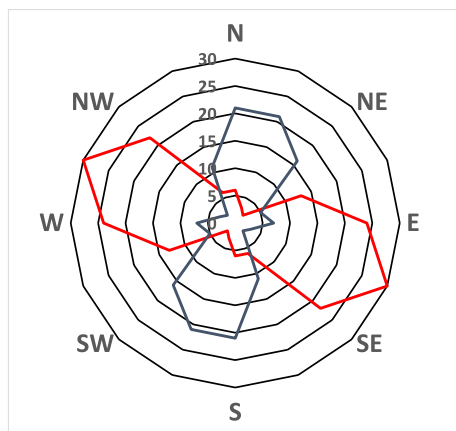


Fig. 3. Distribution of orientations of principal stress axes σ_1 (red line) and σ_3 (blue line) in the study area for the whole dataset combined. Value on radar chart represents the number of measurements.

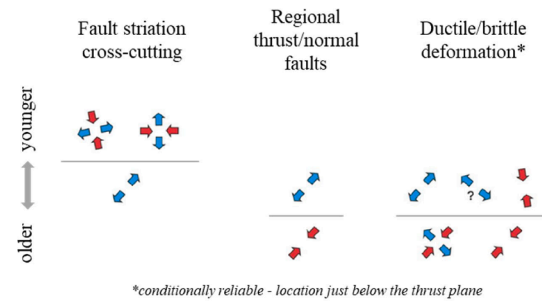


Fig. 4. Relative chronology of determined phases based on field observations (Žibret, 2015). Arrows show orientations of principal stress axes σ_1 (red) and σ_3 (blue).

and Csontos, 2001).

Statistical analysis of paleostress tensor orientations (Fig. 6) showed variations within different blocks. NW-SE directed compression and NE-SW tensions were the main paleostress orientations in block 1. Within block 2 a similar situation occurred, although the orientations were rotated for approximately 15° CCW. E-W compression and N-S tension were determined as the main paleostress orientations in blocks 3 and 4, while in block 5 the main compression direction was NNE-SSW and the main tension direction WNW-ESE.

4. Discussion

The currently established interpretation of determined orientation of the main paleostress axes made by Žibret (2015) and Žibret and Vrabc (2016) includes four kinematic Cenozoic phases and two Mesozoic ones. Mesozoic phases include Triassic and Jurassic extensions, which corresponds to the separation of Adria plate from Africa. The orientation of principal normal stress vectors corresponds well with the orientation of sin-sediment normal faults in Triassic rocks and Neptunian dykes in the Jurassic lithological units. The oldest among four determined Cenozoic kinematic phases is the Paleogene contraction in the direction of NE-SW (phase 1), which corresponds to the closure of the Vardar ocean and the beginning of convergence of Adria-Apulia microplate with the Eurasian

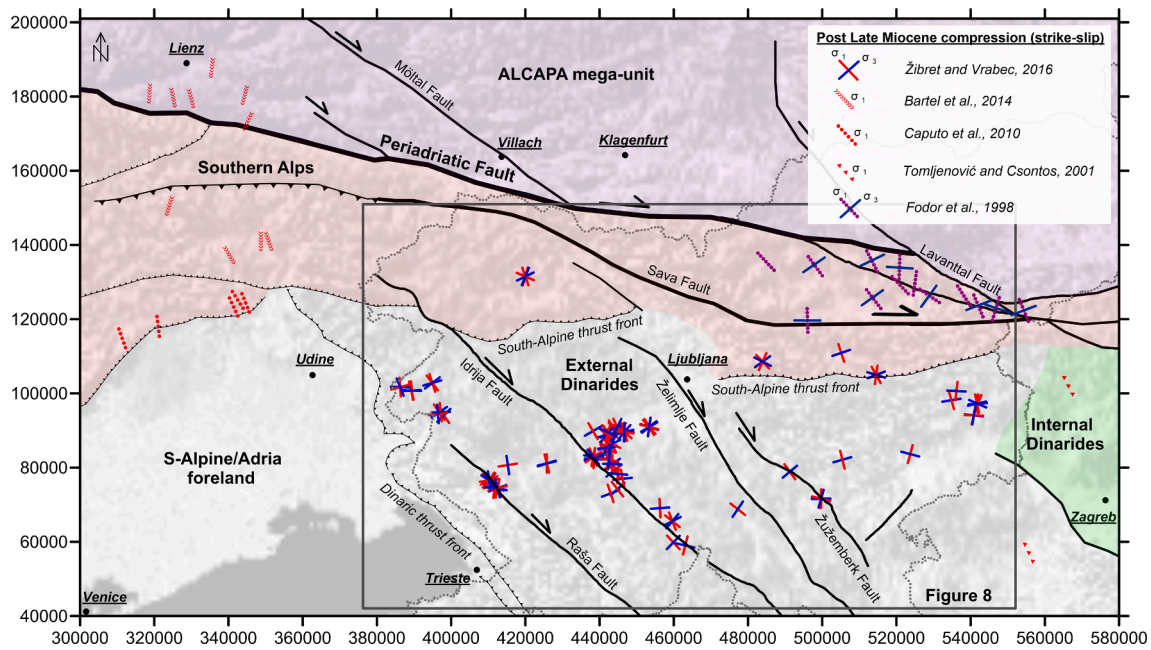


Fig. 5. Orientations of the main stress tensors on a regional scale according to data from this study and literature data.

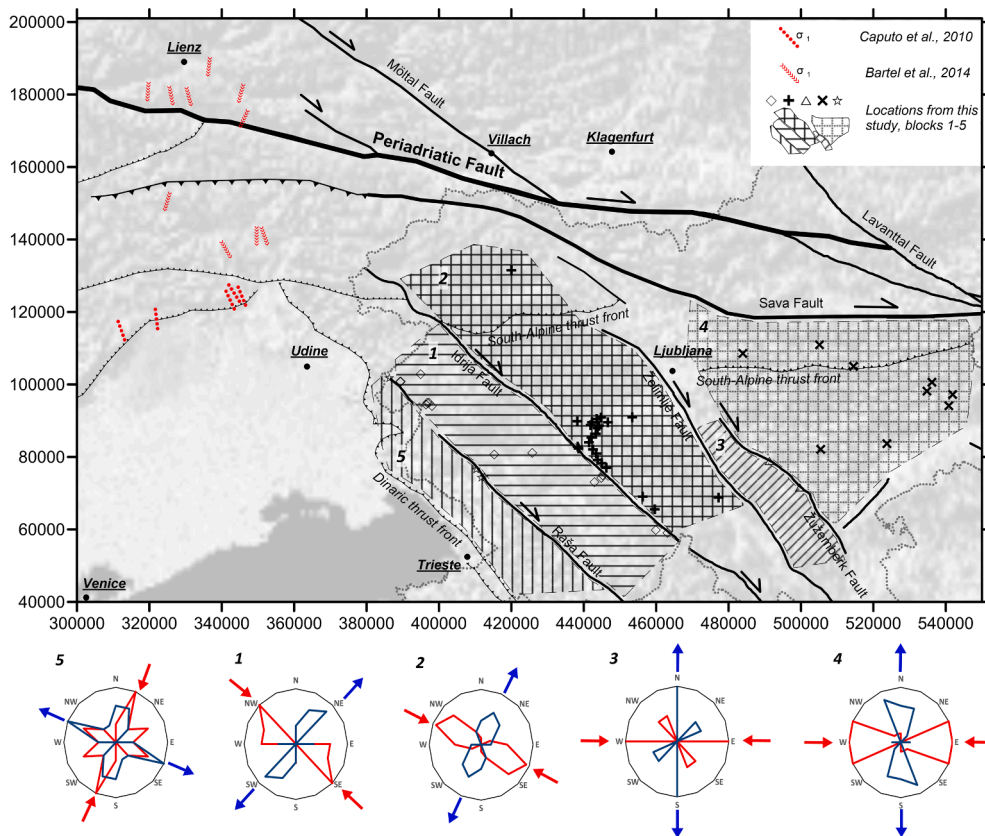


Fig. 6. Results of statistical analysis of paleostress tensor orientation (compression: red line/arrow; tension: blue line/arrow) in different blocks with dominant tensor orientation indication.

plate. A younger phase (phase 2) was interpreted as middle Miocene NE-SW extension, which could correspond with the subduction in Carpathian arch and corresponding back-arc extension in the study area. In the late Miocene an E-W contraction in strike-slip regime was defined as phase 3, which might correspond with the end of subduction in the Carpathian zone. The youngest determined phase (phase 4) is recent N-S

contraction in the strike-slip regime with NW-SE trending dextral faults, which corresponds with the CCW rotation of Adria microplate. However, a number of open questions remain with this established interpretation. The relative age relations between phases were determined during the field observations (Žibret, 2015; Žibret and Vrabc, 2016). Phase 2 is older than phases 4 and 3, and phase 1 is older than phase 2.

All phases can be found in Paleogene rocks, so their age is undoubtable of post-Paleogene age. This study suggests a new interpretation of the paleostress phases, postdating the Middle-Miocene extension (phase 3, phase 4 in Žibret, 2015). Since there were no reliable indicators found during the field work about relative ages between phases 3 and 4 it can be assumed that phases 3 and 4 might occur during the same tectonic process and the deviations of stress orientation could be driven by local block rotations within the regional strike-slip zone of the Dinaric faults. To observe the block rotation the measured fault slip data were divided into smaller groups where we assumed a homogeneous stress field. Low limit values of the compatibility measure ($\geq 15^\circ$) and the dispersion of the Gauss distribution ($\geq 30^\circ$) was set. The fault-slip data, which were attributed to one recent stress state (phase 4; Žibret 2015), were divided into four subgroups of strike-slip stress states (Fig. 7) and one compressional stress state (Fig. 6).

In the initial study (Žibret, 2015) the recent stress state included NNW-SSE compression, which appeared partly in strike-slip and partly in compressional stress regime. In our study we separated data in two phases and observed regional spatial distribution of each phase. The spatial distribution of phase 4 in the territory of Southern Alps in the Sava fault zone (Fodor et al., 1998), NW External Dinarides in Slovenia (Žibret 2015; Žibret and Vrabec 2016), its eastward continuation and Internal Dinarides unit in Croatia (Tomljenović and Csontos, 2001) and its westward/northward continuation in the Southern and Eastern Alps (Bartel et al., 2014; Caputo et al., 2010) is shown in Fig. 7. On the territory of External Dinarides and the Italian Southern Alps phase 1 shows uniform NW-SE compression direction, which indicates that the NNE-SSW compression is the youngest determined stress that was not affected by the block rotation within the Dinaric strike-slip zones. Stress deviation was observed only in the vicinity of the main regional structures, namely Periadriatic fault, Sava fault and South-Alpine thrust front.

Fig. 8 shows four different patterns which are observable within the post Middle-Miocene strike-slip phase data. First, NW-SE directed σ_1 in strike-slip stress regime appears to be uniform within certain areas and seems not to be affected by the regional Dinaric faults (Fig. 8a), similar to the NW-SE directed σ_1 (Fig. 7). This confirms that recent regional stress state in the NW External Dinarides is NW-SE directed compression in compressional or strike-slip stress regime, depending on local structures.

On the other hand, the spatial distribution of \sim E-W compression in strike-slip stress regime (phase 3) is ununiformed (Fig. 8), but strongly corresponds with the most active Dinaric neotectonic zones which was identified by Atanackov et al. (2021): the block between Raša and Idrija fault, the block between Želimlje and Žužemberk fault and the block south of South-Alpine thrust zone (Fig. 7). In the world scientific literature, a block-rotating model in wrench zones is now well-established (Hwang et al., 2008). Wrench faults are a special type of strike-slip faults where the fault plane is vertical, resulting in a more or less straight fault line, as it is the case of Raša, Idrija, Želimlje and Žužemberk faults in the study area. Wrench faults are usually very deep and also include basement rocks. Lozenge-shaped blocks, bounded by R shears and linked to en relais stepping D shears are back-rotating between two parallel strike-slip faults, and the axis of the rotation is always vertical (Harris, 2003). Considering Idrija, Raša and Želimlje fault planes are more or less vertical, crossing various geological structures in approximate straight line, and that block rotation was determined within this study, this could indicate these faults can be attributed as wrench faults.

Statistical analysis revealed variations in paleostress tensor orientations within different blocks (Fig. 6). In the most western area (block 5) between the Dinaric thrust front and the Raša fault the NNE-SSW σ_1 was determined as the dominant stress orientation, with perpendicular oriented σ_3 . However, large variations were detected within this block, which likely occurred because all measurements were used in the case of this block, including those within proximity of the main fault plane. The orientation of the σ_1 within block 5 corresponds very well with the orientation of the Dinaric thrust front in this location, indicating that they are interlinked. This result suggests that Dinaric thrust front in the area is still active today and is a result of the contractional regime E of the Raša fault, likely caused by block rotation within strike-slip faults E of the Dinaric thrust front.

The σ_1 orientation within block 1, which is the main determined active dextral slip zone in the study area according to Atanackov et al. (2021), is NW-SE, while the σ_3 orientation is NE-SW. Very similar, although slightly CCW rotated stress orientation was detected in the area between the Idrija fault and the Želimlje fault (block 2, Fig. 6). On the other hand, the σ_1 orientation within blocks 3 and 4 was approximately E-W with σ_3 approx. S-N (Fig. 6). The recent regional stress in the NW External Dinarides is well defined by GPS measurements (Weber et al.,

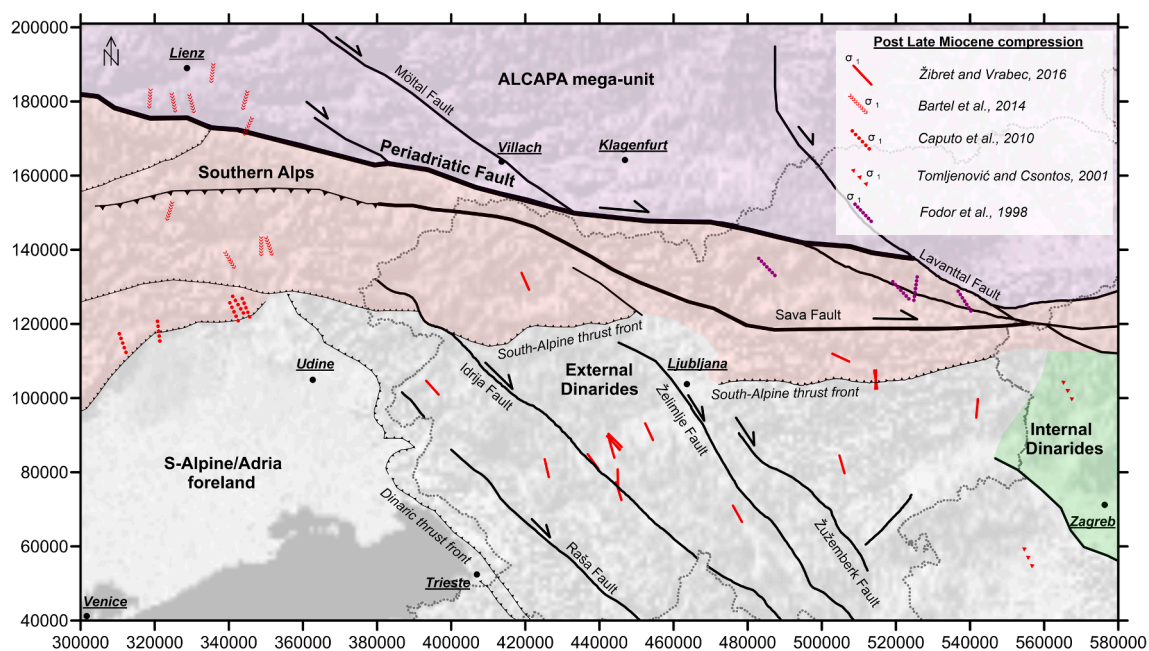


Fig. 7. Orientation of the Alpine phase compression in the region.

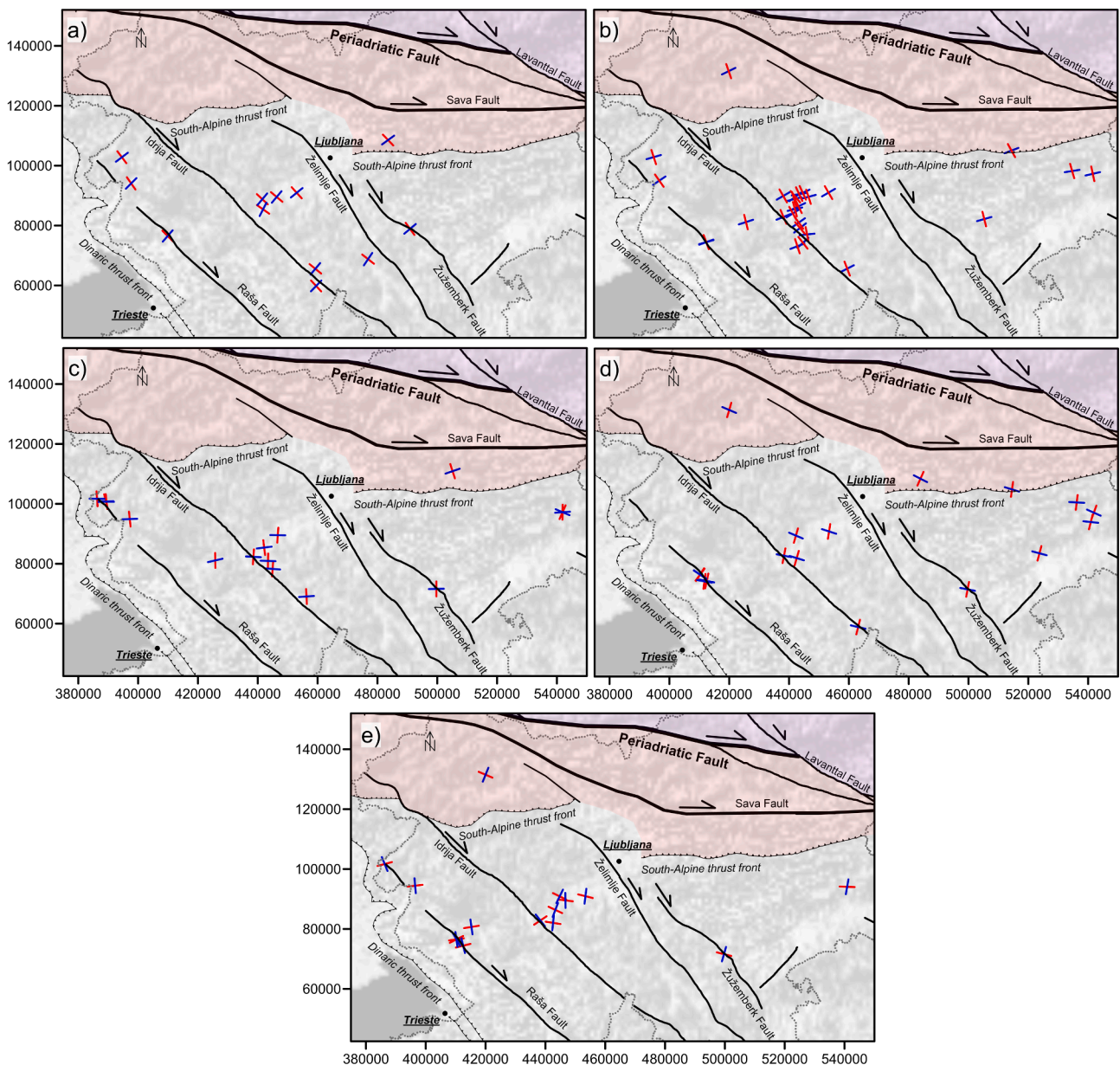


Fig. 8. Regional distribution of the post Middle-Miocene strike-slip compression in the region, divided into 5 separate σ_1 orientations: a) NW-SE; b) NNW-SSE; c) N-S; d) NNE-SSW; e) E-W.

2010), earthquake focal mechanisms (Poljak et al., 2000) and paleostress data (Žibret 2015; Žibret and Vrabc 2016), corresponding to NNW-SSE orientated σ_1 with perpendicular σ_3 in strike-slip stress regime. Fig. 9 shows the difference between recent regional σ_1 orientation and the orientation of σ_1 for blocks 1–5, defined in this study, and CCW rotation angle increase from W towards E, resulting in blocks 1 and 2 (between Raša, Idrija and Želimlje faults) rotating less than blocks 3 and 4 (between Želimlje fault, Žužemberk fault and South Alpine front).

The comparison of stress states on Fig. 8e with the recent stress orientation (Figs. 7 and 8a) shows that the block between the Raša and Idrija faults is less rotated than the block between Idrija and Želimlje faults. Furthermore, the Dinaric fault system between the Raša and Idrija faults is experiencing ~ 2.5 mm/yr dextral slip, while the Dinaric fault system between Idrija and Žužemberk fault only ~ 1 – 2 mm/yr (Atanackov et al., 2021). This could be explained by the proposed block model. In the western blocks (1 and 2) the strike-slip component is dominating, while towards east (blocks 3, 4) the decreased strike-slip component is likely compensated by the increased block rotation,

which is conditioned by regional NE-SW orientated fault system in the eastern part. This finding corresponds well with the measured CCW orientation of underlying Adria microplate (Weber et al., 2010). By combining all above-mentioned observations an improved model of the area can be proposed (Fig. 9), including possible definition of blocks, their CCW rotation and interaction with the neighbouring regional tectonic structures.

5. Conclusions

The re-examination of paleostress data and its spatial analysis from the Adria-Europe collision zone in the NW External Dinarides and Southern Alps improved the existing kinematic model of CCW block rotation between the regional dextral wrenching faults. The results confirm the existence of previously described tectonic blocks in the NW External Dinarides. Statistical analysis of paleostress data from individual blocks between the main regional NW-SE trending faults show CCW rotated main stress axis compared to the recent regional stress

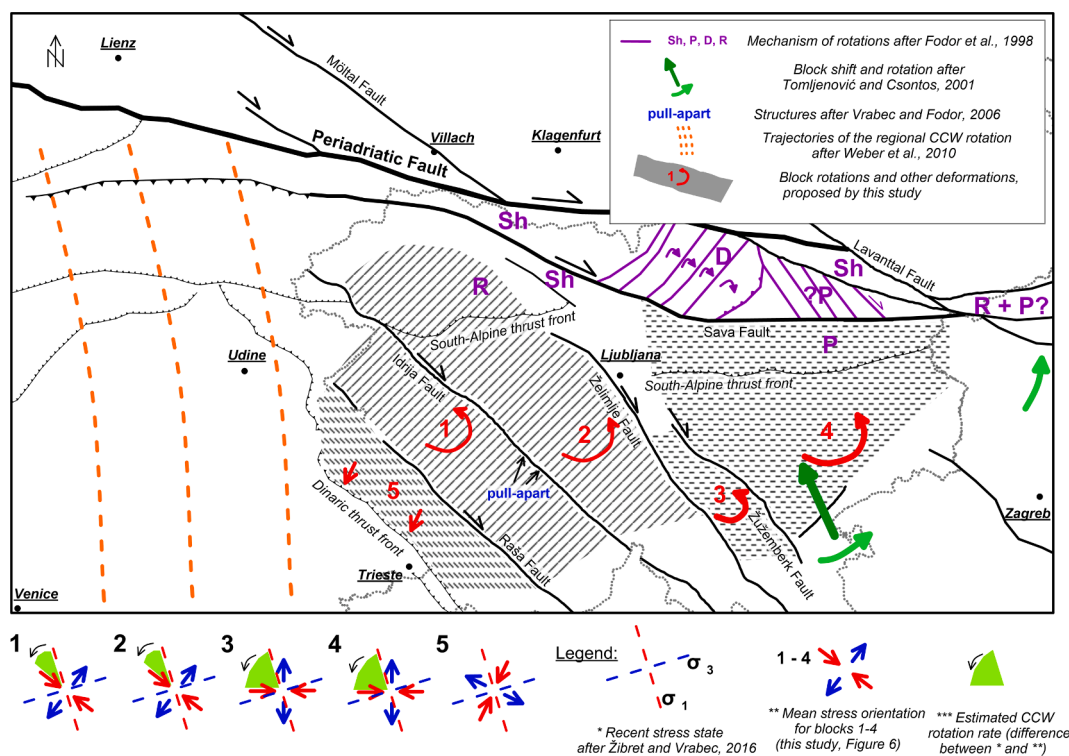


Fig. 9. The proposed model of the rotation of tectonic blocks within the dextral strike-slip faults in the NW External Dinarides, and their interaction with neighbouring regional tectonic structures. Legend: Sh = rotation in shear zone, P = rotation due to pure shear, D = domino-type rotation, R = regional rotation (adopted after (Fodor et al., 1998)).

state. Furthermore, the degree of CCW block rotation decreases from W to E. Namely by increasing distance from the regional wrenching faults with the largest strike-slip component (Raša and Idrija faults) the strike-slip component was compensated by the increased CCW block rotation, limited by regional structures. In a block westward from the main regional NW-SE trending faults the stress orientation suggests that towards Dinaric thrust front the strike slip component is accompanied by NE-SW compression. The kinematic model of block rotation within dextral strike-slip zones was proposed. The results can serve as additional information for seismic hazard assessments as well as they will contribute to the better understanding of kinematics of the collisional zones.

Funding

This work was supported by the Slovenian Research Agency [research core fundings No. P1-0025 and P2-0273].

CRediT authorship contribution statement

L. Žibret: Conceptualization, Methodology, Formal analysis, Writing – original draft. **G. Žibret:** Conceptualization, Methodology, Formal analysis, Writing – original draft, Funding acquisition.

Declaration of Competing Interest

The authors declare that they have no known competing financial interests or personal relationships that could have appeared to influence the work reported in this paper.

Data availability

We have shared the link to the data from PhD thesis in Supplement 1. Detailed information on paleostress data, collected in Pokljuka area are

presented as Supplement 2.

Acknowledgement

Authors would like to thank doc. dr Špela Goričan from PIIR ZRC SAZU for supporting field work in Pokljuka area and Emil Pučko, who kindly checked and corrected the language of this manuscript.

Appendix A. Supplementary data

Supplementary data to this article can be found online at <https://doi.org/10.1016/j.jseae.2023.105723>.

References

- Anderson, H., Jackson, J., 1987. Active tectonics of the Adriatic Region. *Geophys. J. Int.* 91, 937–983. <https://doi.org/10.1111/j.1365-246X.1987.tb01675.x>.
- Atanackov, J., Jamšek Rupnik, P., Jež, J., Celarc, B., Novak, M., Milanič, B., Markelj, A., Bavec, M., Kastelic, V., 2021. Database of Active Faults in Slovenia: Compiling a New Active Fault Database at the Junction Between the Alps, the Dinarides and the Pannonian Basin Tectonic Domains. *Front. Earth Sci.* 9, 604388 <https://doi.org/10.3389/feart.2021.604388>.
- Axen, G.J., 1988. The geometry of planar domino-style normal faults above a dipping basal detachment. *J. Struct. Geol.* 10, 405–411. [https://doi.org/10.1016/0191-8141\(88\)90018-1](https://doi.org/10.1016/0191-8141(88)90018-1).
- Bartel, E.M., Neubauer, F., Genser, J., Heberer, B., 2014. States of paleostress north and south of the Periadriatic fault: Comparison of the Drau Range and the Friuli Southalpine wedge. *Tectonophysics* 637, 305–327. <https://doi.org/10.1016/j.tecto.2014.10.019>.
- Brückl, E., Behm, M., Decker, K., Grad, M., Guterch, A., Keller, G.R., Thybo, H., 2010. Crustal structure and active tectonics in the Eastern Alps: ACTIVE TECTONICS IN THE EASTERN ALPS. *Tectonics* 29. <https://doi.org/10.1029/2009TC002491>.
- Caputo, R., Poli, M.E., Zanferrari, A., 2010. Neogene-Quaternary tectonic stratigraphy of the eastern Southern Alps, NE Italy. *J. Struct. Geol.* 32, 1009–1027. <https://doi.org/10.1016/j.jsg.2010.06.004>.
- Channell, J.E.T., 1996. Palaeomagnetism and palaeogeography of Adria. *SP* 105, 119–132. <https://doi.org/10.1144/GSL.SP.1996.105.01.11>.
- Csontos, L., Nagymarosy, A., 1998. The Mid-Hungarian line: a zone of repeated tectonic inversions. *Tectonophysics* 297, 51–71. [https://doi.org/10.1016/S0040-1951\(98\)00163-2](https://doi.org/10.1016/S0040-1951(98)00163-2).

- Dal Cin, M., Böhm, G., Buseti, M., Picotti, S., Zgur, F., Camerlenghi, A., 2022. 3D velocity-depth model from multichannel seismic in the Dinaric foredeep of the Gulf of Trieste (Adriatic Sea), at the NE edge of Adria plate. *Tectonophysics* 838, 229470. <https://doi.org/10.1016/j.tecto.2022.229470>.
- Doblas, M., 1998. Slickenside kinematic indicators. *Tectonophysics* 295, 187–197. [https://doi.org/10.1016/S0040-1951\(98\)00120-6](https://doi.org/10.1016/S0040-1951(98)00120-6).
- Faccenna, C., Becker, T.W., Auer, L., Billi, A., Boschi, L., Brun, J.P., Capitanio, F.A., Funicello, F., Horváth, F., Jolivet, L., Piomallo, C., Royden, L., Rossetti, F., Serpelloni, E., 2014. Mantle dynamics in the Mediterranean: MEDITERRANEAN DYNAMIC. *Rev. Geophys.* 52, 283–332. <https://doi.org/10.1002/2013RG000444>.
- Fodor, L., Jelen, B., Márton, E., Skaberne, D., Čar, J., Vrabec, M., 1998. Miocene-Pliocene tectonic evolution of the Slovenian Periadriatic fault: Implications for Alpine-Carpathian extrusion models. *Tectonics* 17, 690–709. <https://doi.org/10.1029/98TC01605>.
- Galadini, F., Poli, M.E., Zanferrari, A., 2005. Seismogenic sources potentially responsible for earthquakes with $M \geq 6$ in the eastern Southern Alps (Thiene-Udine sector, NE Italy). *Geophys. J. Int.* 161, 739–762. <https://doi.org/10.1111/j.1365-246X.2005.02571.x>.
- Goričan, S., Žibret, L., Košir, A., Kukoč, D., Horvat, A., 2018. Stratigraphic correlation and structural position of Lower Cretaceous flysch-type deposits in the eastern Southern Alps (NW Slovenia). *Int. J. Earth Sci. (Geol. Rundsch)* 107, 2933–2953. <https://doi.org/10.1007/s00531-018-1636-4>.
- Grützner, C., Aschenbrenner, S., JamsšekRupnik, P., Reichert, K., Saifelislam, N., Vičić, B., Vrabec, M., Welte, J., Ustaszewski, K., 2021. Holocene surface-rupturing earthquakes on the Dinaric Fault System, western Slovenia. *Solid Earth* 12, 2211–2234. <https://doi.org/10.5194/se-12-2211-2021>.
- Hancock, P.L. (Ed.), 1994. *Continental deformation*, first ed. Pergamon Press, Oxford; New York.
- Handy, M.R., Ustaszewski, K., Kissling, E., 2015. Reconstructing the Alps–Carpathians–Dinarides as a key to understanding switches in subduction polarity, slab gaps and surface motion. *Int. J. Earth Sci. (Geol. Rundsch)* 104, 1–26. <https://doi.org/10.1007/s00531-014-1060-3>.
- Harris, L.B., 2003. Folding in high-grade rocks due to back-rotation between shear zones. *J. Struct. Geol.* 25, 223–240. [https://doi.org/10.1016/S0191-8141\(02\)00024-X](https://doi.org/10.1016/S0191-8141(02)00024-X).
- Heberer, B., Reverman, R.L., Fellin, M.G., Neubauer, F., Dunkl, I., Zattin, M., Seward, D., Genser, J., Brack, P., 2017. Postcollisional cooling history of the Eastern and Southern Alps and its linkage to Adria indentation. *Int. J. Earth Sci. (Geol. Rundsch)* 106, 1557–1580. <https://doi.org/10.1007/s00531-016-1367-3>.
- Herak, D., Herak, M., Tomljenović, B., 2009. Seismicity and earthquake focal mechanisms in North-Western Croatia. *Tectonophysics* 465, 212–220. <https://doi.org/10.1016/j.tecto.2008.12.005>.
- Homberg, C., Hu, J.C., Angelier, J., Bergerat, F., Lacombe, O., 1997. Characterization of stress perturbations near major fault zones: insights from 2-D distinct-element numerical modelling and field studies (Jura mountains). *J. Struct. Geol.* 19, 703–718. [https://doi.org/10.1016/S0191-8141\(96\)00104-6](https://doi.org/10.1016/S0191-8141(96)00104-6).
- Hwang, B.-H., Son, M., Yang, K., Yoon, J., 2008. Tectonic Evolution of the Gyeongsang Basin, Southeastern Korea from 140 Ma to the Present, Based on a Strike-Slip and Block Rotation Tectonic Model. *Int. Geol. Rev.* 50, 343–363.
- Kastelic, V., Vrabec, M., Cunningham, D., Gosar, A., 2008. Neo-Alpine structural evolution and present-day tectonic activity of the eastern Southern Alps: The case of the Ravne Fault, NW Slovenia. *J. Struct. Geol.* 30, 963–975. <https://doi.org/10.1016/j.jsg.2008.03.009>.
- Kastelic, V., Vannoli, P., Burrato, P., Fracassi, U., Tiberti, M.M., Valensise, G., 2013. Seismogenic sources in the Adriatic Domain. *Mar. Pet. Geol.* 42, 191–213. <https://doi.org/10.1016/j.marpetgeo.2012.08.002>.
- Kim, Y.-S., Peacock, D.C.P., Sanderson, D.J., 2003. Mesoscale strike-slip faults and damage zones at Marsalforn, Gozo Island, Malta. *J. Struct. Geol.* 25, 793–812. [https://doi.org/10.1016/S0191-8141\(02\)00200-6](https://doi.org/10.1016/S0191-8141(02)00200-6).
- Kissel, C., Laj, C., 1989. *Paleomagnetic Rotations and Continental Deformation*. Springer, Netherlands, Dordrecht.
- Le Breton, E., Handy, M.R., Molli, G., Ustaszewski, K., 2017. Post-20 Ma Motion of the Adriatic Plate: New Constraints From Surrounding Orogens and Implications for Crust-Mantle Decoupling: Post-20 Ma Motion of the Adriatic Plate. *Tectonics* 36, 3135–3154. <https://doi.org/10.1002/2016TC004443>.
- Márton, E., Fodor, L., Jelen, B., Márton, P., Rifejli, H., Kevrić, R., 2002. Miocene to Quaternary deformation in NE Slovenia. *J. Geodyn.* 34, 627–651. [https://doi.org/10.1016/S0264-3707\(02\)00036-4](https://doi.org/10.1016/S0264-3707(02)00036-4).
- Márton, E., Drobne, K., Čosović, V., Moro, A., 2003. Palaeomagnetic evidence for Tertiary counterclockwise rotation of Adria. *Tectonophysics* 377, 143–156. <https://doi.org/10.1016/j.tecto.2003.08.022>.
- Márton, E., Čosović, V., Imre, G., Velki, M., 2022. Changing directions of the tectonic structures, consistent paleomagnetic directions at the NE imbricated margin of Stable Adria. *Tectonophysics* 843, 229594. <https://doi.org/10.1016/j.tecto.2022.229594>.
- Mccaffrey, R., 2013. Crustal Block Rotations and Plate Coupling, in: Stein, S., Freymueller, J.T. (Eds.), *Geodynamics Series*. American Geophysical Union, Washington, D. C., pp. 101–122. <https://doi.org/10.1029/GD030p0101>.
- Monegato, G., Poli, M.E., 2015. Tectonic and Climatic Inferences from the Terrace Staircase in the Meduna Valley, Eastern Southern Alps, NE Italy. *Quat. res.* 83, 229–242. <https://doi.org/10.1016/j.yqres.2014.10.001>.
- Neubauer, F., Cao, S., 2021. Migration of Late Miocene to Quaternary alkaline magmatism at the Alpine-Pannonian transition area: Significance for coupling of Adria plate motion with the Alpine-Carpathian front. *Global Planet. Change* 201, 103491. <https://doi.org/10.1016/j.gloplacha.2021.103491>.
- Petit, J.P., 1987. Criteria for the sense of movement on fault surfaces in brittle rocks. *J. Struct. Geol.* 9, 597–608. [https://doi.org/10.1016/0191-8141\(87\)90145-3](https://doi.org/10.1016/0191-8141(87)90145-3).
- Picha, F.J., 2002. Late orogenic strike-slip faulting and escape tectonics in frontal Dinarides-Hellenides, Croatia, Yugoslavia, Albania, and Greece. *Bulletin* 86. <https://doi.org/10.1306/61EEDD32-173E-11D7-8645000102C1865D>.
- Placer, L., 2008. Principles of the tectonic subdivision of Slovenia. *Geologija* 51, 205–217. <https://doi.org/10.5474/geologija.2008.021>.
- Placer, L., Čar, J., 1997. Structure of Mt. Blegoš between the Inner and the Outer Dinarides. *Geologija* 40, 305–323. <https://doi.org/10.5474/geologija.1997.016>.
- Poljak, M., Živčić, M., Zupančič, P., 2000. The Seismotectonic Characteristics of Slovenia: Pure appl. geophys. 157, 37–55. <https://doi.org/10.1007/PL00001099>.
- Ratschbacher, L., Frisch, W., Linzer, H.-G., Merle, O., 1991. Lateral extrusion in the eastern Alps, PART 2: Structural analysis. *Tectonics* 10, 257–271. <https://doi.org/10.1029/90TC02623>.
- Schmid, S.M., Pfiffner, O.A., Froitzheim, N., Schönborn, G., Kissling, E., 1996. Geophysical-geological transect and tectonic evolution of the Swiss-Italian Alps. *Tectonics* 15, 1036–1064. <https://doi.org/10.1029/96TC00433>.
- Schmid, S.M., Scharf, A., Handy, M.R., Rosenberg, C.L., 2013. The Tauern Window (Eastern Alps, Austria): a new tectonic map, with cross-sections and a tectonometamorphic synthesis. *Swiss J. Geosci.* 106, 1–32. <https://doi.org/10.1007/s00015-013-0123-y>.
- Schmid, S.M., Fügenschuh, B., Kounov, A., Mačenco, L., Nievergelt, P., Oberhänsli, R., Pleuger, J., Schefer, S., Schuster, R., Tomljenović, B., Ustaszewski, K., van Hinsbergen, D.J.J., 2020. Tectonic units of the Alpine collision zone between Eastern Alps and western Turkey. *Gondw. Res.* 78, 308–374. <https://doi.org/10.1016/j.gr.2019.07.005>.
- Serpelloni, E., Vannucci, G., Anderlini, L., Bennett, R.A., 2016. Kinematics, seismotectonics and seismic potential of the eastern sector of the European Alps from GPS and seismic deformation data. *Tectonophysics* 688, 157–181. <https://doi.org/10.1016/j.tecto.2016.09.026>.
- Sperner, B., Zweigel, P., 2010. A plea for more caution in fault-slip analysis. *Tectonophysics* 482, 29–41. <https://doi.org/10.1016/j.tecto.2009.07.019>.
- Stojadinović, U., Krstekanić, N., Matenco, L., Bogdanović, T., 2022. Towards resolving Cretaceous to Miocene kinematics of the ADRIA-EUROPE contact zone in reconstructions: Inferences from a structural study in a critical Dinarides area. *Terra Nova* 34, 523–534. <https://doi.org/10.1111/ter.12618>.
- Tari, V., 2002. Evolution of the northern and western Dinarides: a tectonostratigraphic approach. *Stephan Mueller Spec. Publ. Ser.* 1, 223–236. <https://doi.org/10.5194/smsps-1-223-2002>.
- Tojlić, M., Matenco, L., Ducea, M.N., Stojadinović, U., Milivojević, J., Đerić, N., 2013. The evolution of a key segment in the Europe-Adria collision: The Fruška Gora of northern Serbia. *Global Planet. Change* 103, 39–62. <https://doi.org/10.1016/j.gloplacha.2012.10.009>.
- Tomljenović, B., Csontos, L., 2001. Neogene-Quaternary structures in the border zone between Alps, Dinarides and Pannonian Basin (Hrvatsko zagorje and Karlovac Basins, Croatia). *Int J Earth Sci* 90, 560–578. <https://doi.org/10.1007/s005310000176>.
- Ustaszewski, K., Kounov, A., Schmid, S.M., Schaltegger, U., Krenn, E., Frank, W., Fügenschuh, B., 2010. Evolution of the Adria-Europe plate boundary in the northern Dinarides: From continent-continent collision to back-arc extension: ADRIA-EUROPE PLATE BOUNDARY, DINARIDES. *Tectonics* 29. <https://doi.org/10.1029/2010TC002668>.
- van Gelder, I.E., Matenco, L., Willingshofer, E., Tomljenović, B., Andriessen, P.A.M., Ducea, M.N., Beniest, A., Gručić, A., 2015. The tectonic evolution of a critical segment of the Dinarides-Alps connection: Kinematic and geochronological inferences from the Medvednica Mountains, NE Croatia. *Tectonics* 34, 1952–1978. <https://doi.org/10.1002/2012TC003937>.
- Vrabec, M., Fodor, L., 2006. Late cenozoic tectonics of Slovenia: structural styles at the Northeastern corner of the Adriatic microplate. In: Pinter, N., Gyula, G., Weber, J., Stein, S., Medak, D. (Eds.), *The Adria Microplate: GPS Geodesy, Tectonics and Hazards*, Nato Science Series: IV: Earth and Environmental Sciences. Kluwer Academic Publishers, Dordrecht, pp. 151–168. https://doi.org/10.1007/1-4020-4235-3_10.
- Wallace, L.M., 2004. Subduction zone coupling and tectonic block rotations in the North Island, New Zealand. *J. Geophys. Res.* 109, B12406. <https://doi.org/10.1029/2004JB003241>.
- Weber, J., Vrabec, M., Pavlovčić-Prešeren, P., Dixon, T., Jiang, Y., Stopar, B., 2010. GPS-derived motion of the Adriatic microplate from Istria Peninsula and Po Plain sites, and geodynamic implications. *Tectonophysics* 483, 214–222. <https://doi.org/10.1016/j.tecto.2009.09.001>.
- Žalohar, J., Vrabec, M., 2007. Paleostress analysis of heterogeneous fault-slip data: The Gauss method. *J. Struct. Geol.* 29, 1798–1810. <https://doi.org/10.1016/j.jsg.2007.06.009>.
- Žibret, L., 2015. *Kinematic and paleostress evolution of the NW-SE trending Dinaric faults in the northwestern External Dinarides* (doctoral thesis). University of Ljubljana, Ljubljana.
- Žibret, L., Vrabec, M., 2016. Paleostress and kinematic evolution of the orogen-parallel NW-SE striking faults in the NW External Dinarides of Slovenia unraveled by mesoscale fault-slip data analysis. *Geol. Cro* 69, 295–305. <https://doi.org/10.4154/geol.2016.30>.
- Zoback, M.D., Zoback, M.L., Mount, V.S., Suppe, J., Eaton, J.P., Healy, J.H., Oppenheimer, D., Reasenber, P., Jones, L., Raleigh, C.B., Wong, I.G., Scotti, O., Wentworth, C., 1987. New Evidence on the State of Stress of the San Andreas Fault System. *Science* 238, 1105–1111. <https://doi.org/10.1126/science.238.4830.1105>.